Numerical simulation and noise prediction of the aerial propeller

Liu Yang [a], Jun Huang [b], Mingxu Yi [c], Chaopu Zhang [d], Hao Song [e] and Qian Xiao [f]

School of Beihang University, Beijing 100191, China

[a]loisy66@163.com, [b]junhuang1964@163.com, [c]yimingxu88@163.com, [d]zhangchaopu@buaa.edu.cn, [e]songhao@buaa.edu.cn, [f]xiao_qian@buaa.edu.cn

Abstract. In this paper, the aerodynamic and acoustic performances of an aerial propeller are evaluated. In the aerodynamic analysis, the RANS (Reynolds-averaged Navier–Stokes) method combined with CFD (Computational Fluid Dynamics) technique is used. The acoustic analysis is based on Farassat 1A which derived from FW-H (Ffowcs Williams-Hawkings) equation. The pressure of the aerodynamic analysis is given as the input of the acoustic calculation. The acoustic analysis also draws some meaningful conclusions.

Keywords: Aerial propeller; Aerodynamic characteristics; Noise prediction; Farassat 1A.

1. Introduction

Aerial propeller is an aircraft instrument which can transform the power of the aerial engine into thrust. With the outbreak of the oil crisis in the Middle East in 1970s, aerial propeller comes to play a more and more important role in regional aircraft, general aviation and especially UAV (Unmanned Aerial Vehicle). Aerial propeller owns good performance at subsonic speed, as well as supersonic with supercritical aerofoil.

One critical problem of aerial propeller propulsion system is noise and vibration, comparing with jet propulsion system. Aerial propeller noise not only affects the surrounding environment, but also increases the structural vibration and acoustic fatigue, thereby reducing safety of aircraft.

Aerial propeller noise prediction method includes two processes: obtaining aerial propeller aerodynamic performance and calculating sound radiation by setting the blades surface pressure distribution as acoustic source. This approach has been widely adopted in calculating the noise of rotor [1, 2], axial fan [3] and marine propeller [4-8]. Also splendid results have been achieved. However, at aerial propeller calculation area, this hybrid method is barely used.

In this article, RANS method and Lighthill's acoustic analogy are used to predict the noise of aerial propeller. Firstly, a method of CFD technique based on MRF (Moving Reference Frame) is applied here to investigate the aerodynamic performance of the propeller. Then, radiated noise of aerial propeller is predicted through solving FW-H equation. Results of aerodynamic performance from simulation and experiments are compared to ensure the accuracy. And several useful conclusions have been made.

2. Governing Equations

2.1 Aerodynamic.

The RANS (Reynolds-averaged Navier-Stokes) in rotating coordinate system is adopted here to calculate the flow filed.

$$\frac{\partial}{\partial t}\iiint_V \vec{W} dV + \iint_{\partial V}\left[F(\vec{W}) - G(\vec{W})\right]\bullet \vec{n}\, dS = \iiint_V \vec{Q} dV \tag{1}$$

$\vec{W} = [\rho, \rho u, \rho v, \rho w, \rho E]^T$; ρ is density of the fluid, u, v, w is velocity components of fluid, E is internal energy of unit fluid, $\vec{n}$ is normal vector, $F(\vec{W})$, $G(\vec{W})$ is viscous flux and inviscid flux, respectively. $\vec{Q}$ Is additional part causing by rotation.

2.2 Acoustic.

The Formulation of Farassat 1A based on the FW-H equation is used to calculate the aerodynamic noise.

$$p'(x,t) = p'_T(x,t) + p'_L(x,t) \tag{2}$$

With

$$4\pi p'_T(x,t) = \int_S \left[\frac{\rho_0 \dot{v}_n}{r(1-M_r)^2} \right]_{ret} dS + \int_S \left[\frac{\rho_0 v_n (r\dot{M}_i \hat{r}_i + c_0 M_r - c_0 M^2)}{r^2(1-M_r)^3} \right]_{ret} dS \tag{3}$$

$$\begin{aligned} 4\pi p'_L(x,t) = \frac{1}{c_0} \int_S \left[\frac{\dot{l}_i \hat{r}_i}{r(1-M_r)^2} \right]_{ret} dS + \int_S \left[\frac{l_r - l_i M_i}{r^2(1-M_r)^2} \right]_{ret} dS \\ + \frac{1}{c_0} \int_S \left[\frac{l_r (r\dot{M}_i \hat{r}_i + c_0 M_r - c_0 M^2)}{r^2(1-M_r)^3} \right]_{ret} dS \end{aligned} \tag{4}$$

Where $p'_T(x,t)$ the thickness is noise and $p'_L(x,t)$ is the load noise.

3. Numerical Simulation

The geometric data and geometric model of aerial propeller we explored is showed below.

Table 1Geometrical data of aerial propeller

Subject	Measurements
Diameter	0.960m
Chord width	0.117m
Pitch angle	66degree

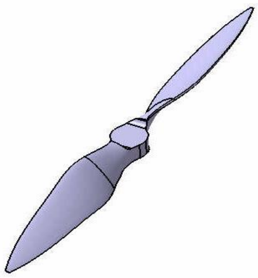

Fig. 1 Geometric model of aerial propeller

The computational domain is divided into two regions: independent rotational domain for model and outer stationary domain for flow. Using a cylinder, with its diameter of D (D denotes the diameter of the propeller) and length of propeller's height, divided the solution domain into rotating part and static part. In rotating domain, the grid is unstructured tetrahedral volume as well as refined (shown in **Fig.2**), whereas far-field blocks consist of structured hexahedra (shown in **Fig.2**).

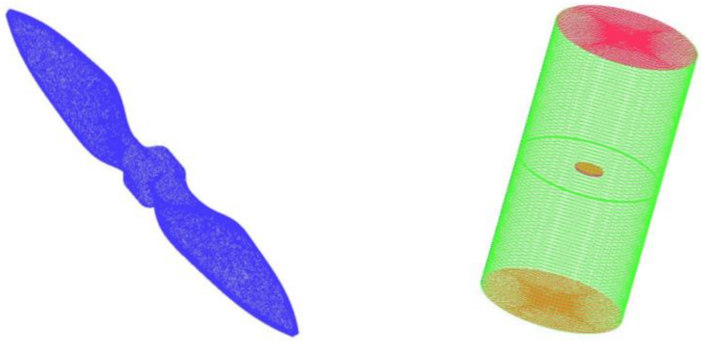

Fig. 2 Grid of aerial propeller

The flow simulation is carried out by using solution technique implemented in ANSYS Fluent, based on the RANS equations. The selected boundary conditions are: velocity-inlet for inlet zone, outlet-vent for outlet zone, wall on aerial propeller, and matching interfaces for message exchange between two domains. The calculation is carried on (Standard, Realizable) turbulence model. The SIMPLEC discretization schemes are used to discretize the equations of pressure–velocity coupling. Time-step is assembled with the period of aerial propeller.

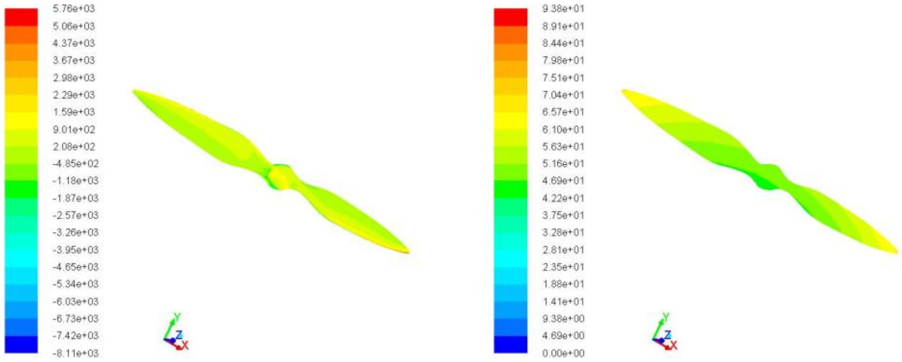

Fig. 3 Pressure (left) and velocity (right) distribution of the propeller at 900rpm

The contours indicate that the pressure at leading edge of the blade is higher than the trailing edge's, whereas the velocity distribution of propeller is at symmetric state.

The acoustic analysis and calculation are showed as follows. The main component of propeller noise is rotation noise. Rotation noise consists of thickness noise caused by monopole source and load noise caused by dipole source. The sound pressure is expressed as dB (decibels) while predicted SPLs (Sound Pressure Levels) is given by:

$$SPLs = 20\lg\frac{P_p}{P_r} \tag{5}$$

Predicted pressure is given by P_p . Reference pressure is given by P_r and equals to $2\times$10-5Pa.

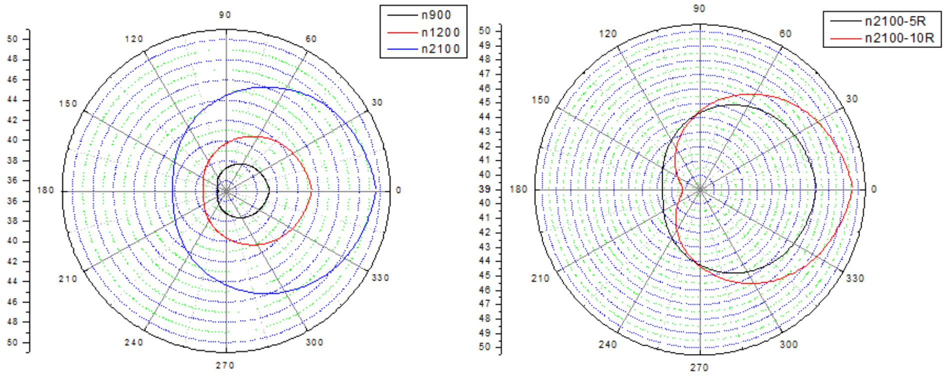

Fig. 4 Directivity of SPLs of thickness noise in different situations

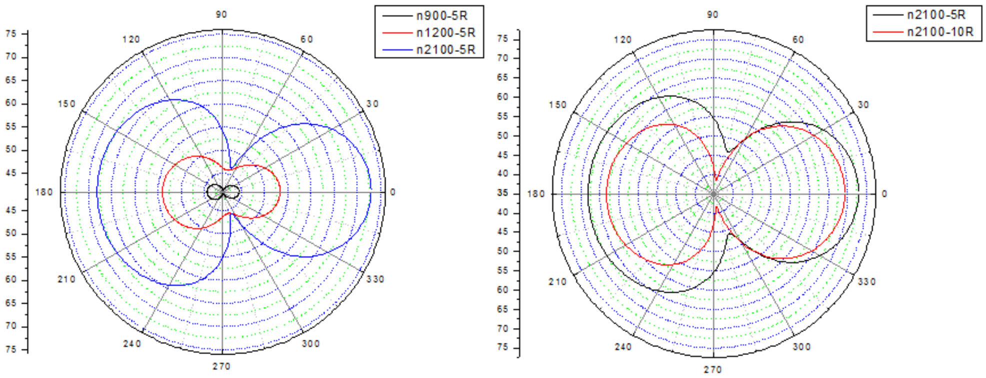

Fig. 5 Directivity of SPLs of load noise in different situations

The directivity of SPLs of thickness noise for various rotary speeds and observation distances are presented in **Fig.4-5**. The rotary speeds in **Fig.4** are 900rpm, 1200rpm and 2100rpm at observation distance of 5R (R denotes the radius of the propeller), respectively. It can be concluded that with the increase of rotary speed, SPLs of the propeller rise simultaneously. The observation distances of propeller at rotary speed of 2100rpm in Fig.10 are 5R and 10R, respectively. It can be found that SPLs of the propeller decline with increase of observation distance.

The thickness noise of aerial propeller shows obvious characteristics of monopole sound source. And the load noise shows obvious characteristics of dipole sound source. As the rotational speed goes up, the thickness noise and the load noise both increase. But the increase of load noise is lower than thickness noise's. With the increase of the observe distance, the thickness noise and the load noise both reduced dramatically.

4. Conclusion

The CFD method based on MRF model is used here to investigate aerodynamic performance. We can confirm that CFD method in pre-calculation is rather desirable.

Using Farassat 1A based on FW-H equation can predict the propeller noise effectively. Though the analysis of noise, it can be found that noise of the propeller increases as rotary speed raises. And in the noise of propeller, thickness noise accounts for a major proportion. Thickness noise is mainly influenced by aerodynamic shape of the propeller, which has mentioned above.

From the directivity of SPLs, we can ensure that the thickness noise is higher than load noise, which indicating that thickness noise occupies a dominant position in propeller noise.

References

[1] HAN Zhong-hua, SONG Wen-ping, QIAO Zhi-de. Aeroacoustic Calculation for Helicopter Rotor in Hover and in Forward Flight Based on FW-H Equation [J]. ACTA AERONAUTICA ET ASTRONAUTICA SINICA, 2003, 24(5): 400-404.

[2] Fan F, Shi Y J, and Xu G H. Computational research on aerodynamic and aeroacoustic characteristics of scissors tail-rotor in hover. Acta Aeronautica et Astronautica Sinica, 2013, 34(9): 2100-2109.

[3] Hu B, OuYang H, Wu Y, et al. Numerical prediction of the interaction noise radiated from an axial fan [J]. Applied Acoustics, 2013, 74(4): 544-552.

[4] Lam W H, Hamill G A, Robinson D J. Initial wash profiles from a ship propeller using CFD method [J]. Ocean Engineering, 2013, 72: 257-266.

[5] Califano A, Steen S. Numerical simulations of a fully submerged propeller subject to ventilation [J]. Ocean engineering, 2011, 38(14): 1582-1599.

[6] Ji B, Luo X, Peng X, et al. Numerical analysis of cavitation evolution and excited pressure fluctuation around a propeller in non-uniform wake[J]. International Journal of Multiphase Flow, 2012, 43: 13-21.

[7] GONG Jing-feng ZHANG Wen-ping MING Ping-jian XUAN Ling-kuan. Numerical Analysis of the Propeller Low Frequency Flow-Noise [J]. Chinese Journal of Ship Research, 2012, 7(5).

[8] Lee K J, Bae J H, Kim H T, et al. A performance study on the energy recovering turbine behind a marine propeller [J]. Ocean Engineering, 2014, 91: 152-158.